Preferred orientation of microcracks or liquid inclusion, or individual minerals may cause such an anisotropy of the S-wave[11,13-15]. At present, it is difficult to interpret the anisotropy. We, however, hypothesize that this anisotropy is related to a magma reservoir because AMJ, KTJ and TAK are located near volcanoes inside the volcanic front[16] (Fig. 1). It seems possible, therefore, that S-waves from the deep earthquakes pass through deep magma reservoirs beneath volcanoes (Fig. 3). If thin elliptical inclusions trending north–south exist within magma reservoirs, then a velocity anisotropy of S-waves could be caused with the maximum velocity axis NS.

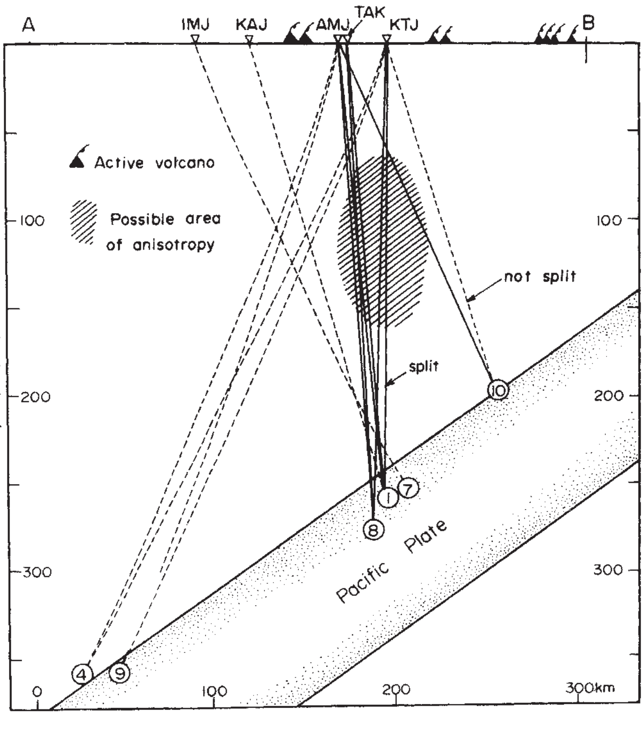

Fig. 3 S-wave ray paths for earthquakes 1, 4, 7, 8 and 10 projected on the plane A–B (Fig. 1). Solid rays denote those associated with the S-wave splitting (arrival time difference >0.4 s). A possible area of anisotropy is inferred from a combination of these ray paths.

We thank the Observation Center for Earthquake Prediction, Nagoya University and the Hokuriku Observatory of Kyoto University for providing the seismographic records and use of their facilities, and Professors K. Aki and S. Crampin, and Mr F. Yamazak for helpful comments.

Received 11 February; accepted 30 April 1980.

1. Kumazawa, M., Helmstaedt, H. & Masaki, K. *J. geophys. Res.* **76,** 1231–1247 (1971).
2. Christensen, N. I. *Bull. geol. Soc. Am.* **82,** 1681–1694 (1971).
3. Ewing, W. M., Jadetsky, W. S. & Press, F. *Elastic Waves in Layered Media* (McGraw-Hill, New York, 1957).
4. Morris, G. B., Raitt, R. W. & Shor, G. G. *J. geophys. Res.* **74,** 3095–3109 (1969).
5. Bamford, D. *Geophys J. R. astr. Soc.* **49,** 29–48 (1977).
6. Okada, H. *et al. J. Phys. Earth* **26,** Suppl. s491–s502 (1978).
7. Hirn, A. *Geophys. J. R. astr. Soc.* **49,** 49–58 (1977).
8. Suyehiro, S., Ichikawa, M. & Tsumura, K. *J. Phys. Earth* **25,** Suppl. s69–s78 (1977).
9. Kamitakara Crustal Movement Observatory and Research Section for Earthquake Prediction *Bull. Disaster Prev. Inst., Kyoto Univ.* **21,** 119–135 (1978).
10. Aoki, H. *J. Phys. Earth* **22,** 229–290 (1971).
11. Nur, A. & Simmons, G. *J. geophys. Res.* **74,** 6669–6674 (1969).
12. Ichikawa, M. & Mochizuki, E. *Pap. Meteor. Geophys. Jap. Meteor. Ag.* **22,** 229–290 (1971).
13. Birch, F. *J. geophys. Res.* **65,** 1083–1102 (1960); **66,** 2199–2224 (1961).
14. Christensen, N. L. & Ramananantoandro, *J. geophys. Res.* **76,** 4003–4010 (1971).
15. Todd, T., Simmons, G. & Baldridge, W. S. *Bull. seis. Soc. Am.* **63,** 2007–2020 (1973).
16. Matsuda, T., Nakamura, K. & Sugimura, A. *Tectonophysics* **4,** 349–366 (1967).
17. Isshiki, N., Matsui, K. & Ono, K. *Selected Bibliography of Japanese Volcanoes* (Japan Geological Survey, 1968).
18. Utsu, T. *Kagaku (Science), Tokyo* **44,** 739–746 (1944).

Restrictions on the compositions of mid-ocean ridge basalts: a fluid dynamical investigation

Herbert E. Huppert

Department of Applied Mathematics and Theoretical Physics, University of Cambridge,

R. Stephen J. Sparks

Department of Earth Sciences, University of Cambridge, Downing Place, Cambridge CB2 3EW, UK

The nature of the melts parental to mid-ocean ridge basalts has been vigorously debated. Opinions vary between those considering the parental magma to be magnesia-rich (picritic basalt) with 15–20% MgO and those arguing that the parental melts are compositionally related to the most primitive liquids erupted at mid-ocean ridges (MgO ~ 9–11%). This difference of between 5 and 11% in MgO content represents a temperature interval of 100–250 °C. The actual MgO content places constraints on the thermal conditions at the mantle source. The high-magnesia liquid theory is supported by melting experiments on mantle and basalt samples[1–3] and by petrological studies of ophiolite complexes[4]. However, this theory does not seem to be immediately consistent with the fact that no glasses or aphyric rocks of these compositions have ever been sampled from the sea floor. Indeed the most primitive glass compositions that occur as inclusions in olivine megacrysts and as glassy margins to pillow lavas have MgO contents in the range 9–11%. Models of generating low MgO partial melts from the mantle have been proposed. For example, Presnall *et al.*[5] consider that melting at cusps in the peridotite mantle solidus could generate such melts. We outline here a fluid dynamical model for a basaltic mid-ocean ridge magma chamber supplied by high-magnesia melt from the mantle. The model predicts that high-magnesia extrusives will not be erupted, that ultramafic cumulates should occur at the base of the oceanic crust, that lava compositions will be restricted to MgO contents <10% and that magma mixing will be a common feature of sea-floor basalts[6].

Before presenting the model we emphasize a fundamental feature of the moderate to low pressure evolution of picritic to tholeiitic basalt by crystal fractionation[7]. Figure 1 shows the dependence of density of high-magnesia melts on MgO content as crystallization occurs, calculated by the method of Bottinga and Weill[8]. As an example, we use the estimate of Elthon[4] for the parent magma for the oceanic crust (MgO ~ 17·8%) and generate successive residual liquids by crystallization of olivine (Fo_{90}). As olivine crystallizes out the density of the residual liquid decreases despite the declining temperature. The residual liquid reaches the density minimum *A* and the liquid joins a cotectic (perhaps olivine-plagioclase or olivine–plagioclase–pyroxene). Subsequent crystallization, dominated by plagioclase and pyroxene, generates residual liquids of progressively increasing density, due to iron-enrichment accompanied by low degrees of silica enrichment. Similar relationships between density and composition have been documented from several suites of mid-ocean ridge basalts[7], although the exact position of the minimum point *A* may change slightly from case to case. The variation of magma density with composition is complicated by the effects of suspended crystals, but in general the effect of suspended crystals will accentuate the relationships shown in Fig. 1 (ref. 7) by increasing the magma density at a fixed temperature.

It is significant that the most primitive glasses yet recovered from the sea floor occupy the density minimum shown in Fig. 1 (9–11% MgO)[6,7,9,10]. Mid-ocean ridge basalts are all more

0028-0836/80/270046-03$01.00

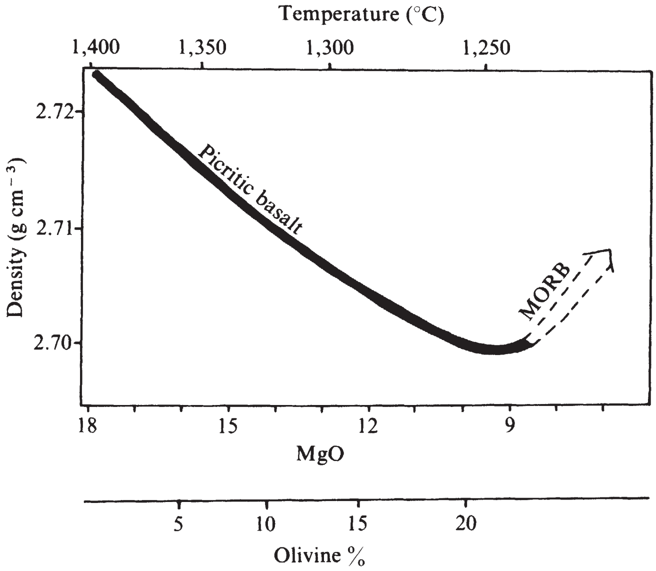

Fig. 1 Variation of melt density with MgO content in picritic liquids. The estimate of Elthon[4] is used as an example of the parental magma to the ocean crust with MgO ~ 17.8% and generated a succession of liquid compositions down to MgO = 10% by removal of forsterite (Fo_{90}). The approximate percentage of olivine removed in generating the successive liquids is indicated by the lower scale. Liquidus temperatures were estimated approximately from the experimental data of Krishnamurthy and Cox[17]. The density minimum at *A* is illustrated with the approximate trend of mid-ocean ridge basalt density with MgO content for MgO < 9% (after ref. 7).

evolved than this composition and show abundant evidence for mixing between evolved liquids and more primitive liquids (with MgO 9–11%)[6,9–11].

Figure 2 shows our model of a magma chamber containing typical mid-ocean ridge basalt into which a new influx of hot, but denser, picritic-basalt melt is intruded. The concept of an open-system magma chamber periodically replenished by new melt from depth[12] is now widely accepted as the most probable situation existing beneath the mid-ocean ridges, although the exact geometry and location of mid-ocean ridge magma chambers is still uncertain[13]. The temperature contrast between the two magmas may be 100–200 °C, depending largely on the MgO content of the picritic basalt. Investigations of an analogous system[14] where a hot salty layer of water underlies a cold freshwater layer indicates that the dense fluid will remain at the base of the chamber. Between the two layers there is a non-turbulent interface across which heat and salt are transferred by molecular rather than turbulent processes. Unless the densities of the two layers are virtually identical, no physical mixing occurs across the interface, although each layer convects vigorously. We suggest that this form of motion can also occur in magmas where the ratio of diffusivity of mass to that of heat is typically $< 10^{-5}$.

We have adapted the empirical and theoretical results of studies on the salt/water system to the picrite/basalt system in a magma chamber. A detailed treatment of the problem, which has several geological implications in addition to the situation described here, will be presented elsewhere. We summarize here the results pertinent to the problems of mid-ocean ridge magma genesis. Vigorous convection occurs in the two layers (Fig. 2*b*) and heat transfer through the interface between the two layers results in rapid cooling of the lower layer.

Our calculations indicate that the temperature of the lower layer as a function of time, $T(t)$, can be expressed as

$$T(t) = T(0) + \{[\Delta^{-7/3} + 7\,A(0.5 + r)t/3] - \Delta\}/(1 + 2r)$$

where $T(0)$ is the initial temperature, Δ is the initial temperature difference between the layers and r is the ratio of the thickness of the lower layer to that of the upper layer. The expression takes account of the heat of crystallization for olivine using a value of 200 cal g^{-1}. The constant A is dependent on the physical properties of the fluids.

$$A = 0.32(g\kappa^2\alpha^7/\nu)^{1/3}/(h\sigma^2)$$

where g is the gravitational acceleration, κ is the thermal diffusivity, α is the coefficient of thermal expansion, ν is the kinematic viscosity, h is the thickness of the lower layer and σ is the density contrast between the layers due to the difference in MgO contect divided by the mean density.

Typical values of the physical properties are: $\kappa = 10^{-6}$ m^2 s^{-1}; $\alpha = 5 \times 10^{-5}$ K^{-1}; $\nu = 10^{-3}$ m^2 s^{-1}; $\sigma = 2 \times 10^{-2}$. Figure 3 shows the cooling history of the lower layer for values of h between 3 and 300 m with an upper layer thickness of 4 km, an initial upper layer temperature of 1,255 °C and an initial lower layer temperature of 1,385 °C. We observe that the lower layer cools to thermal equilibrium with the upper layer in a time scale of a few months to a few years. The reason for the rapid cooling rates is the intense turbulent convection that occurs for large Rayleigh numbers[14]. Typically, the initial Rayleigh number of the lower layer exceeds 10^9.

Another consequence of the turbulently convecting flow regime is that olivines precipitated from the lower picrite layer will be kept in turbulent suspension throughout the cooling of the lower layer. In all plausible models we calculate that the mean turbulent velocities[15] are in the range 1–5 cm s^{-1}, whereas the free-fall velocities of olivine crystals of 1–5 mm diameter (typical dimensions in ultramafic cumulates and olivine–phyric lavas) in magnesia-rich liquids are in the range 10^{-2}–10^{-3} cm s^{-1}. The olivine settling rates only become comparable to the turbulent velocities when the temperature difference becomes small (< 1 °C).

The model predicts (Fig. 2) that the lower picritic basalt will not mix with the upper basalt layer and that it will cool rapidly in

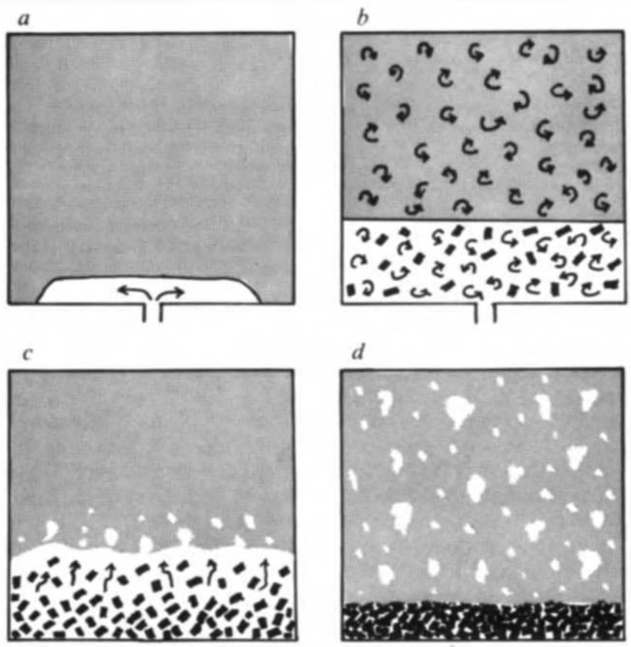

Fig. 2 Schematic model for the behaviour of a new influx of picritic melt into a MOR magma chamber (not to scale): *a*, intrusion of hot, dense picrite into reservoir of fractionating basalt; *b*, stable stratification into two layers which equilibrate thermally by turbulent convection with growth of olivine in lower layer; *c*, convection dies in lower layer at the end of cooling history allowing for olivine settling and separation of low density interstitial basaltic melt; *d*, Cumulate olivine layer formed at base of chamber as low density interstitial melt mixes convectively with heated upper layer.

a period of a few years at most. During its cooling to thermal equilibrium with the upper layer, the picrite will be highly turbulent and olivines precipitated from the liquid will remain in suspension until a late stage when the temperatures of the two layers are nearly equal. Provided that the upper layer is volumetrically large, the lower layer will transform into a mixture of suspended olivine in a basalt liquid. This basaltic liquid will be more primitive than the upper layer which has increased slightly in temperature. In many of our calculations, the residual liquid composition in the lower layer is estimated to occur near to the density minimum shown in Fig. 1. Note that the lower layer will in fact increase in bulk density as it crystallizes, as long as the olivines are kept in suspension. For example, the bulk density of liquid A plus 20% olivines in suspension is 2.82 g cm^{-3}. The dense lower layer remains in existence as long as the convection is sufficiently vigorous to suspend the olivine crystals.

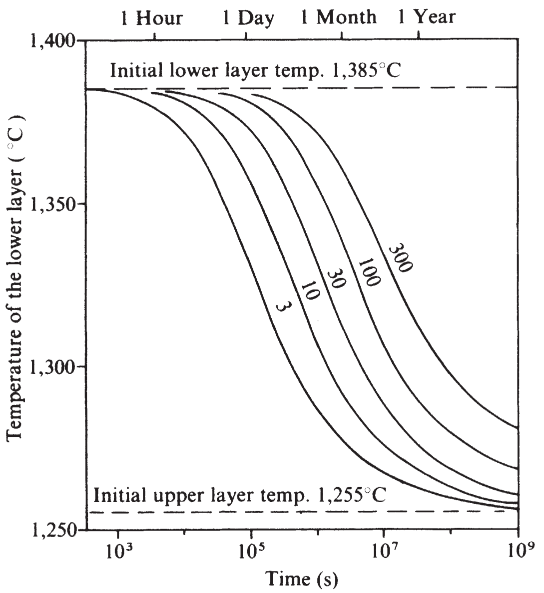

Fig. 3 Temperature of the lower layer as a function of time for various thicknesses (h) in metres of the lower layer for an upper layer 4 km thick.

Once convection has died down in the closing stages of cooling, theory[16] predicts a concentration gradient of olivines will be generated in the lower layer when the free-fall velocity and convective velocities become comparable (Fig. 2c). Only a slight concentration gradient is required to nullify completely the density instability caused by the slight temperature gradient at this late stage, leading to a transition to stable stratification of the lower layer. We predict that the layer will pass rapidly to a stage of *en masse* sedimentation of suspended olivine. A substantial amount of basaltic liquid will segregate as the olivines sediment (Fig. 2c). For example, if a picrite layer, 100 m thick, contained 18% MgO at 1,400 °C and the upper layer, 2,000 m thick, contained basalt with MgO = 9% at 1,250 °C, the lower layer would evolve to a suspension of 20% olivines in a basalt liquid at an equilibrium temperature of 1,264 °C and 10% MgO. Sedimentation of the olivine to a dense close-packed mode (60% olivine) would liberate ~80% of the remaining basaltic liquid, generating a cumulate layer 33 m thick (Fig. 2d). The olivines would be relatively uniform in composition as they have grown in conditions approximating equilibrium crystallization in the turbulent layer. Such features are found in the homogeneous olivine cumulates observed at the base of ophiolites. Further adcumulus growth (as is common in ultramafic cumulates) would drive out further basaltic liquid component.

Thermal equilibration between the two layers (Fig. 2) would require that the upper layer has increased in temperature. In many cases the upper layer would be more evolved and denser than the basalt liquid derived from the lower layer as illustrated in the example calculation above. We conclude that the basalt liquid squeezed out during olivine sedimentation in the lower layer will be buoyant in the upper layer and will mix with it convectively (Fig. 2d). In this way the compositions of basalts which can erupt at the surface are restricted in composition as they periodically become mixed with basalt close to the density minimum.

We thank G. M. Brown, C. H. Donaldson, D. P. MacKenzie, R. K. O'Nions, E. R. Oxburgh and J. S. Turner for helpful comments. Contribution no. 49 (Department of Earth Sciences, University of Cambridge).

Received 11 March; accepted 28 April 1980.

1. O'Hara, M. J. *Earth Sci. Rev.* **4,** 69 (1968).
2. Green, D. H., Hibberson, W. O. & Jaques, A. L. in *The Earth: its Origin, Structure and Evolution*, 265 (ed. McElhinny, E.) (1979).
3. Clarke, D. B. & O'Hara, M. J. *Earth planet. Sci. Lett.* **44,** 153 (1979).
4. Elthon, D. *Nature* **278,** 514 (1978).
5. Presnall, D. C., Dixon, J. R., O'Donnell, T. M. & Dixon, S. A. *J. Petrol.* **20,** 3 (1979).
6. Dungan, M. A. & Rhodes, J. M. *Contr. Miner. Petrol.* **67,** 417 (1978).
7. Sparks, R. S. J., Meyer, P. C. & Sigurdsson, H. *Earth planet. Sci. Lett.* **46,** 419 (1980).
8. Bottinga, Y. & Weill, D. F. *Am. J. Sci.* **269,** 169 (1970).
9. Donaldson, C. H. & Brown, R. W. *Earth planet. Sci. Lett.* **37,** 81 (1977).
10. Bryan, W. B. *J. Petrol.* **20,** 293 (1979).
11. Walker, D., Shibata, T. & DeLong, S. E. *Contr. Miner. Petrol.* **70,** 111 (1979).
12. O'Hara, M. J. *Nature* **266,** 503 (1977).
13. Nisbet, E. G. & Fowler, C. M. R. *Geophys. J. R. astr. Soc.* **54,** 631 (1978).
14. Turner, J. S. *Buoyancy Effects in Fluids* (Cambridge University Press, 1979); *A. Rev. Fluid Mech.* **6,** 37–56 (1974).
15. Townsend, A. A. *The Structure of Turbulent Shear Flow* (Cambridge University Press, 1976).
16. Batchelor, G. K. *2nd Austr. Conf. on Hydraulics and Fluid Mechanics* 19–41 (1965).
17. Krishnamurthy, P. & Cox, K. G. *Contr. Miner. Petrol.* **62,** 53 (1977).

Volcanic rocks cored on Hess Rise, western Pacific Ocean

T. L. Vallier*, K. E. Windom†, K. E. Seifert† & Jörn Thiede‡

* US Geological Survey, Menlo Park, California 94025
Department of Earth Sciences, Iowa State University, Ames, Iowa 50011
Institutt for Geologi, Universitet i Oslo, Norway

Large aseismic rises and plateaus in the western Pacific include the Ontong–Java Plateau, Magellan Rise, Shatsky Rise, Mid-Pacific Mountains, and Hess Rise. These are relatively old features that rise above surrounding sea floors as bathymetric highs. Thick sequences of carbonate sediments overlie, what are believed to be, Upper Jurassic and Lower Cretaceous volcanic pedestals. We discuss here petrological and tectonic implications of data from volcanic rocks cored on Hess Rise. The data suggest that Hess Rise originated at a spreading centre in the late early Cretaceous (Aptian–Albian stages). Subsequent off-ridge volcanism in the late Albian–early Cenomanian stages built a large archipelago of oceanic islands and seamounts composed, at least in part, of alkalic rocks. The volcanic platform subsided during its northward passage through the mid-Cretaceous equatorial zone. Faulting and uplift, and possibly volcanism, occurred in the latest Cretaceous (Campanian–Maastrichtian stages). Since then, Hess Rise continued its northward movement and subsidence. Volcanic rocks from holes drilled on Hess Rise during IPOD Leg 62 (Fig. 1) are briefly described here and we relate the petrological data to the origin and evolution of that rise. These are the first volcanic rocks reported from Hess Rise.

Hess Rise is a triangular-shaped bathymetric high that is bounded on the west by the Emperor Seamount chain, on the north-east by the Emperor Trough, and on the south by the Mendocino Fracture Zone. A clear sequence of magnetic anomalies has not been discovered on Hess Rise, but it is believed to lie entirely within the Cretaceous magnetic quiet